Kaposi's Sarcoma–Associated Herpesvirus Confers a Survival Advantage to Endothelial Cells

Ling Wang and Blossom Damania

Department of Microbiology and Immunology and Lineberger Comprehensive Cancer Center,
University of North Carolina at Chapel Hill, Chapel Hill, North Carolina

Abstract

Kaposi's sarcoma–associated herpesvirus (KSHV) is associated with three different human malignancies, including Kaposi's sarcoma (KS), primary effusion lymphoma, and multicentric Castleman's disease. The KS lesion is of endothelial cell in origin and is highly dependent on autocrine and paracrine factors for survival and growth. In this study, we show that KSHV infection of endothelial cells induces the activation of the prosurvival phosphatidylinositol 3-kinase (PI3K)/Akt/mammalian target of rapamycin pathway. KSHV infection of endothelial cells augmented cell survival in the presence of apoptotic inducers, including etoposide and staurosporine, and under conditions of serum deprivation. We found that KSHV infection of endothelial cells also increased the ability of these cells to form an *in vitro* tubular network under conditions of stress and growth factor deprivation. Finally, we show that the nuclear factor-κB and PI3K pathways are also required for endothelial tubular network formation. Collectively, these results suggest that KSHV infection of endothelial cells modulates cell signaling pathways and induces cell survival and angiogenesis, thereby contributing to the pathogenesis induced by KSHV. [Cancer Res 2008; 68(12):4640–8]

Introduction

Kaposi's sarcoma (KS)–associated herpesvirus (KSHV/HHV-8) is a gammaherpesvirus first identified from KS biopsies (1). Since its discovery, KSHV has been found in all epidemiologic forms of KS, and viral genomic DNA is present in AIDS-associated KS as well as HIV-negative classic and transplant-associated KS (2). KSHV is also linked to two lymphoproliferative diseases: primary effusion lymphomas (PEL) and multicentric Castleman's disease (3, 4).

Angiogenesis is the formation of new blood vessels from a preexisting microvascular network. Angiogenesis is important for many normal physiologic processes such as organ development and wound healing (5). Many tumors usurp this process, and angiogenesis is central for tumor growth and metastasis.

KS is a highly inflammatory and angiogenic vascular tumor with characteristic spindle cells that are of endothelial origin. The KS lesion has been shown to express high levels of vascular endothelial growth factor (VEGF) and fibroblast growth factor (bFGF/FGF-2), which are necessary for the maintenance of the lesion (6). Furthermore, antiangiogenic therapies are currently being used for treatment of KS (7).

The angiogenic potential of several genes of KSHV has also been investigated. KSHV G protein–coupled receptor (vGPCR) is a homologue of human interleukin-8 (IL-8) receptor and can induce constitutive, ligand-independent signaling activity. Signaling by vGPCR results in elaboration of many mitogenic and angiogenic cytokines that are vital to KSHV biology and KSHV-driven malignancies. vIL6, a homologue of human IL-6, has also been implicated in the development of tumorigenesis and angiogenesis (8). Our recent studies have shown that the K1 protein of KSHV induces the secretion of VEGF, matrix metalloproteinase-9, and also enhances angiogenesis and tumor size *in vivo* (9).

The phosphatidylinositol 3-kinase (PI3K)/Akt signaling pathway plays an important role in cell growth and survival. PI3K is a heterodimer composed of a catalytic subunit (p110) and an adaptor/regulatory subunit (p85), which are activated by receptor activation. PI3K activation leads to Akt activation and phosphorylation on threonine 308 and serine 473 (10). Akt is a critical regulator of PI3K-mediated cell survival and it phosphorylates and inactivates several proapoptotic proteins, including members of the forkhead family of transcription factors (FKHR/FOXO) and glycogen synthase kinase-3β (11, 12). Activated Akt also enhances protein synthesis by increasing the phosphorylation of the mammalian target of rapamycin (mTOR; ref. 13). As a serine/threonine protein kinase, mTOR has been shown to regulate cell growth, proliferation, motility, survival, protein synthesis, and gene transcription (14). Akt can activate mTOR in different ways. First, Akt has been shown to directly phosphorylate and activate mTOR (15). Second, it can activate mTOR through phosphorylation and inhibition of tuberous sclerosis complex 2 (TSC 2), which is a negative regulator of mTOR (16). Third, Akt can modulate mTOR activity through the regulation of cellular ATP levels, which leads to the inactivation of AMP-activated protein kinase (AMPK) and TSC 2 (17).

We have previously shown that the KSHV K1 protein activates the PI3K/Akt/mTOR pathway in B cells and endothelial cells (9, 18). Similarly, KSHV vGPCR has also been found to up-regulate the PI3K/Akt/mTOR pathway (19–21). These studies were performed with individual KSHV viral genes, and in this article, we examined the role of PI3K/Akt/mTOR activation on endothelial cell survival in the context of the whole virus.

Here, we report that KSHV infection of endothelial cells enhances angiogenesis, activates the PI3K/Akt/mTOR pathway, and inactivates AMPK. We find that this activation of the PI3K/Akt cell survival pathway in endothelial cells infected by KSHV confers a survival advantage and protects infected cells from apoptosis.

Materials and Methods

rKSHV.219 production. Vero cells containing latent rKSHV.219 (KSHV-Vero) and a recombinant baculovirus KSHV Orf50 (BacK50) were kindly provided by Dr. Jeffrey Vieira (Department of Laboratory Medicine, University of Washington, Seattle, WA; ref. 22). rKSHV.219 expresses green fluorescent protein (GFP) from the EF-1α promoter and puromycin

resistance gene as a selectable marker. The insect SF9 cells were grown in Grace's insect medium (Life Technologies) supplied with 10% fetal bovine serum (FBS) at 28°C in a 5% CO_2 incubator. Three days after BacK50 infection, the baculovirus-containing supernatant was separated from SF9 cells by centrifugation (3,500 rpm for 10 min). KSHV-Vero cells were infected with BacK50 and treated with 1 mmol/L sodium butyrate. At 65 to 72 h postinfection, the medium was harvested and cells were removed by centrifugation (3,500 rpm for 10 min). Supernatants were passed through a 0.45-μm filter.

Infection of endothelial cells. Primary human umbilical vein endothelial cells (HUVEC) from Clonetics were cultured in sterile endothelial growth medium (EGM-2, Clonetics) with 10% FBS and were maintained at 37°C in a 5% CO_2 environment. Immortalized HUVEC were made by infecting primary HUVEC with a hTERT-encoding retrovirus that also expressed the hygromycin resistance gene as previously described (23). rKSHV.219 produced from KSHV-Vero cells was used to infect immortalized HUVEC in the presence of 0.8 mg/mL polybrene. After 3 d, the cells were selected in medium containing 0.5 μg/mL puromycin for ~2 wk to select for stable KSHV-HUVEC.

Serum starvation assay. Primary immortalized HUVEC and KSHV-HUVEC (1×10^5) were plated in each well of a six-well plate and cultured in EGM-2 with 10% FBS at 37°C. After 24 h, cells were washed twice with PBS and cultured in endothelial basic medium, EBM-2 (Clonetics), with no serum or supplements in a 37°C incubator for up to 5 d. The images were taken with a Zeiss Axiovert 200 inverted fluorescence microscope. The number of cells in 10 different fields were counted and averaged after trypan blue staining.

Caspase-3 activation assay and poly(ADP)ribose polymerase-1 activity assay. HUVEC and KSHV-HUVEC cells (1×10^6) were seeded in 100-mm dishes. After 24 h, the cells were washed twice with PBS and then treated with EBM-2 medium containing one of the following: DMSO vehicle control, 500 ng/mL tumor necrosis factor α (TNFα; Sigma), 100 μmol/L etoposide (Sigma), or 20 nmol/L staurosporine (Sigma) for 24 h (24, 25). The cells were harvested and a caspase-3 activation assay was performed using the ApoAlert caspase-3 Fluorescent Assay kit (Clontech). A poly(ADP)ribose polymerase-1 (PARP-1) activity assay was also performed using the Universal Colorimetric PARP Assay kit (Trevigen). In addition, the caspase-3 inhibitor, Z-VAD-FMK (Sigma), was used in the caspase-3 activation and PARP-1 assays. In this case, cells were grown in EGM-2 complete medium with 10% FBS and treated with one of the following: DMSO vehicle control, 100 μmol/L etoposide, 100 μmol/L etoposide plus 50 μmol/L Z-VAD-FMK (26), 20 nmol/L staurosporine, or 20 nmol/L staurosporine plus 50 μmol/L Z-VAD-FMK (26) for 24 h. Caspase-3 and PARP-1 activity was measured in the cells using the ApoAlert caspase-3 Fluorescent Assay kit and the Universal Colorimetric PARP-1 Assay kit, respectively.

Western blots. HUVEC and KSHV-HUVEC were seeded and grown in EGM-2 medium, and after 48 h, the cells were washed with ice-cold PBS containing 1 mmol/L Na_3VO_4 and protease inhibitor cocktail (Roche). Cells were lysed in Triton/NP40 lysis buffer. Western blots were performed with the following antibodies: phospho-PI3K p85 antibody (1:2,000 dilution), rabbit phospho-Akt (Ser[473]) antibody (1:1,000 dilution), rabbit phospho-mTOR (Ser[2448]) antibody (1:2,000 dilution) and phospho-AMPK (Thr[172]) antibody (1:1,000 dilution). All of these antibodies were from Cell Signaling Technology.

Tubule formation assays. A KSHV-negative lymphoma cell line, BJAB, and the body-cavity–based lymphoma cell line BCBL-1 were grown in RPMI medium (Cellgro) with 10% FBS. Cells were washed with PBS twice and then incubated in serum-free plain RPMI medium for 48 h at 37°C. The conditioned medium from BJAB and BCBL-1 cells was harvested by centrifugation at 3,500 rpm for 10 min. Growth factor–reduced Matrigel (BD Biosciences) was added to the wells of a prechilled 24-well plate (0.25 mL/well). The plate was placed in a 37°C incubator for 30 min and the Matrigel was allowed to solidify. To determine whether the cells could form tubules in B-cell conditioned medium, 3×10^4 immortalized HUVEC and KSHV-HUVEC were resuspended in either 1 mL plain RPMI medium or conditioned medium from BJAB or BCBL-1 cells and were then plated on the solidified Matrigel. The plate was incubated in a 37°C incubator for

different time points, and images were taken with a Nikon T200 fluorescence microscope. To determine whether the cells could form tubules in the absence of VEGF and FGF, the cells were resuspended in VEGF minus EGM-2 medium or FGF minus EGM-2 medium, plated on the solidified Matrigel and incubated at 37°C for up to 4 d. For the VEGF antibody experiments, HUVEC and KSHV-HUVEC were resuspended in EBM-2 medium or EBM-2 medium containing 20 μg/mL VEGF antibody (Sigma) as previously described (27). The cells were then seeded on Matrigel and incubated at 37°C incubator for16 h. Images were taken with a Nikon T200 fluorescence microscope.

For drug treatment experiments, 3×10^4 immortalized HUVEC and KSHV-HUVEC treated with EBM-2 medium overnight were resuspended in 1 mL EGM-2 medium containing either 50 nmol/L rapamycin (mTOR inhibitor, Calbiochem; ref. 28), 150 μmol/L ciglitazone (AMPK activator, Calbiochem), 2.5 μmol/L SU6656 (Src inhibitor, Sigma; ref. 29), 20 μmol/L piceatannol (Syk inhibitor, Calbiochem; ref. 30), 5 μmol/L Bay11-7085 [nuclear factor-κB (NF-κB) inhibitor, Calbiochem; ref. 31], or 20 μmol/L LY294002 (PI3K inhibitor, Calbiochem; ref. 32). The cells were then plated on the solidified Matrigel. The plate was put in a 37°C incubator for 4 h. The angiogenic index was calculated as the number of branch points in a field for a particular treatment. Five different fields were counted for each treatment and the number of branch points was averaged.

Results

KSHV infection of endothelial cells induces activation of the PI3K/Akt/mTOR pathway and inactivation of AMPK. To obtain KSHV-infected endothelial cells, HUVEC were infected with a recombinant KSHV virus containing a green fluorescent protein (GFP) expression cassette and a puromycin expression cassette (22). After selection with 0.5 μg/mL puromycin for several weeks, we obtained a 100% KSHV-infected stable HUVEC cell line, which is denoted as KSHV-HUVEC.

To determine whether the KSHV-infected endothelial cells displayed an activated PI3K/Akt/mTOR pathway, equal micrograms of HUVEC and KSHV-HUVEC cell lysate were loaded on SDS-PAGE and subjected to Western blot analysis with antibodies directed against components of the PI3K/Akt pathway. KSHV infection of HUVEC resulted in increased phosphorylation of the p85 subunit of PI3K (Fig. 1), indicative of its activation. We also found that there was increased phosphorylation of Akt on serine 473, concomitant with its activation (Fig. 1). mTOR, a downstream target of Akt, also seemed to be more activated in KSHV-infected HUVEC compared with uninfected HUVEC, as evidenced by phosphorylation of serine 2448. Interestingly, AMPK, a negative regulator of mTOR, showed decreased phosphorylation on threonine 172 in KSHV-infected HUVEC (Fig. 1), suggesting that AMPK is less activated in KSHV-infected HUVEC compared with uninfected HUVEC. Thus, the net effect of KSHV infection of endothelial cells is activation of the PI3K/Akt/mTOR pathway and inactivation of AMPK (Fig. 1).

KSHV infection augments endothelial cell survival upon serum deprivation. Because we observed that the PI3K/Akt pathway was activated in KSHV-HUVEC and because this pathway has been associated with cell survival (33, 34), we determined whether the KSHV-infected cells were more resistant to apoptosis induced by serum starvation. We subjected uninfected HUVEC versus KSHV-infected HUVEC to serum starvation using EBM-2 medium without serum or cytokine supplements for various time points. Twenty-four hours after serum starvation, there was no significant difference between the two cell lines, but by 48 hours, some of the uninfected HUVEC died and most of the uninfected HUVEC appeared to be undergoing apoptosis. In contrast, the KSHV-HUVEC appeared healthy (Fig. 2). By 72 hours, >60% of the
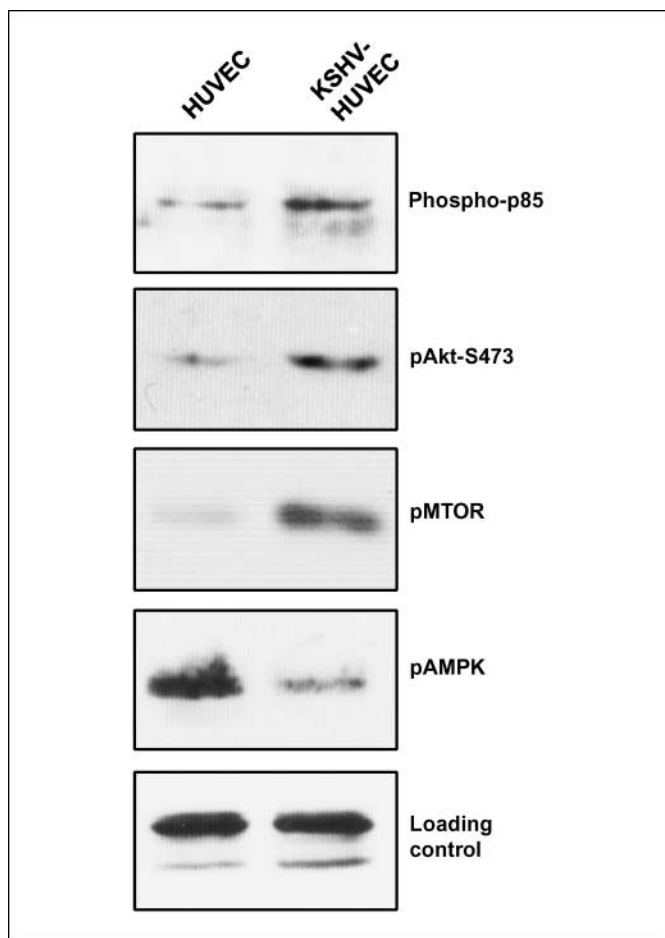
Figure 1. KSHV infection induces activation of the PI3K/Akt/mTOR pathway. HUVEC and KSHV-HUVEC were harvested 48 h postseeding, and equal micrograms of cell lysates were subjected to SDS-PAGE. The gel was transferred to nitrocellulose and Western blots were performed with the indicated antibodies. KSHV infection of endothelial cells increased phosphorylation of the p85 subunit of PI3K, phosphorylation of Akt, and mTOR. We also found that KSHV-HUVEC displayed a decrease in the phosphorylation of AMPK.

that measures the cleavage of the caspase-3 peptide substrate, DEVD–7-amino-4-trifluoromethyl coumarin (DEVD-AFC), resulting in AFC, which could be detected at an emission of 505 nm.

Etoposide inhibits DNA synthesis (36) and staurosporine is a relatively nonselective inhibitor of several protein kinases, including protein kinase C and protein kinase A (37, 38). Both of these drugs have previously been shown to induce cellular apoptosis (24, 25). As shown in Fig. 3A, with the treatment of 100 μmol/L etoposide, the activity of caspase-3 in the uninfected HUVEC was more than twice that of the KSHV-HUVEC, suggesting that KSHV infection of endothelial cells confers a protective effect against etoposide-induced apoptosis. Similarly, activation of caspase-3 in staurosporine-treated KSHV-HUVEC was lower than that seen in staurosporine-treated uninfected HUVEC (Fig. 3A). Together, these data suggest that KSHV infection inhibits endothelial cell apoptosis induced by either etoposide or staurosporine.

Interestingly, TNF-α treatment of either HUVEC or KSHV-HUVEC did not seem to induce much apoptosis in either cell line as measured by caspase-3 activity (Fig. 3A). This has been previously reported for TNF-α exposure of HUVEC (39). A20, a TNF-α–inducible early response zinc finger protein, has been shown to down-regulate NF-κB signaling in HUVEC and also inhibit apoptosis of endothelial cells induced by TNF-α (40, 41). Thus, endothelial cells seem to be resistant to the effects of TNF-α.

Further, to determine whether the apoptosis we observed with etoposide and staurosporine was caspase-3 dependent, we performed caspase-3 activity assays with HUVEC and KSHV-HUVEC in the presence of the caspase-3 inhibitor, Z-VAD-FMK. As shown in Fig. 3B, apoptosis induced by both etoposide and staurosporine was caspase-3 dependent because almost no apoptosis was induced in either HUVEC or KSHV-HUVEC with etoposide or staurosporine in the presence of the caspase-3 inhibitor, Z-VAD-FMK (Fig. 3B).

We also performed PARP-1 activity assays to measure apoptosis. PARP-1 catalyzes the NAD-dependent addition of poly(ADP)-ribose to adjacent nuclear proteins (42). During apoptosis, PARP-1 is specifically cleaved from its enzymatically active form to an inactive form, and the cleavage of PARP has been shown to be a reliable marker for apoptosis in a wide variety of cell types (43). We performed a PARP-1 activity assay using lysates from HUVEC or KSHV-HUVEC treated with etoposide or staurosporine. Higher PARP-1 activity corresponds to lower apoptosis, and, conversely, lower PARP-1 activity corresponds to a higher degree of apoptosis. We found that the PARP-1 activity in HUVEC treated with etoposide or staurosporine was lower than the PARP-1 activity seen in KSHV-HUVEC treated with these same drugs (Fig. 3C). This is consistent with the caspase-3 activity data shown in Fig. 3A. Finally, we also performed the PARP-1 activity assay in the presence of the caspase-3 inhibitor, Z-VAD-FMK (Fig. 3D). The presence of Z-VAD-FMK greatly increased PARP-1 activity in the etoposide- and staurosporine-treated HUVEC and KSHV-HUVEC. In summary, our data indicate that caspase-3–mediated apoptosis by etoposide and staurosporine is much reduced in KSHV-infected HUVEC compared with uninfected HUVEC.

KSHV-infected endothelial cells form tubular networks under conditions of cell stress. The tubule formation assay is an *in vitro* assay for monitoring the formation of capillary-like tubules by endothelial cells and is used to model and measure cell angiogenesis (44). We used growth factor–reduced Matrigel as the basement matrix to induce endothelial cell tubule formation under various conditions. Unlike standard Matrigel, growth factor–reduced

uninfected HUVEC died and had come off the plate. At this time point, most of the KSHV-infected HUVEC still appeared healthy and were attached to the dish. At 96 hours (day 4), there were only a few surviving uninfected HUVEC compared with KSHV-HUVEC. By 120 hours (day 5), almost all of the uninfected HUVEC died. In contrast, ~ 40% of KSHV-HUVEC remained alive at day 5 and maintained normal endothelial cell morphology and behavior (Fig. 2). These results have been repeated four times. Our results suggest that KSHV infection protects endothelial cells under serum starvation conditions.

KSHV infection suppresses etoposide- and staurosporine-induced apoptosis. Next, we determined the ability of uninfected versus KSHV-infected HUVEC to counteract various apoptotic stimuli. HUVEC and KSHV-HUVEC were treated with DMSO (control) or apoptosis inducers, including 500 ng/mL TNF-α, 100 μmol/L etoposide, or 100 nmol/L staurosporine for 24 hours. Caspase-3 is a cysteine protease that has been identified as a key mediator of cell apoptosis and its activation is often used as a hallmark of apoptosis (35). The HUVEC and KSHV-HUVEC cells were harvested and lysed. Equal micrograms of cell lysates were used to perform caspase-3 activation assays using a colorimetric assay

Figure 2. KSHV infection confers endothelial cell survival upon serum deprivation. HUVEC and KSHV-HUVEC were grown in serum-free medium for 5 d. *A,* images of the HUVEC and KSHV-HUVEC cells were taken under bright field microscopy. Additionally, images of the KSHV-HUVEC (which express GFP) were taken under fluorescence microscopy. Time points included were 24, 48, 72, 96, and 120 h after serum starvation. Images shown were taken at ×4 magnification. *B,* graph of the percentage of live cells at different time points. The number of live cells in 10 different fields was counted and averaged.
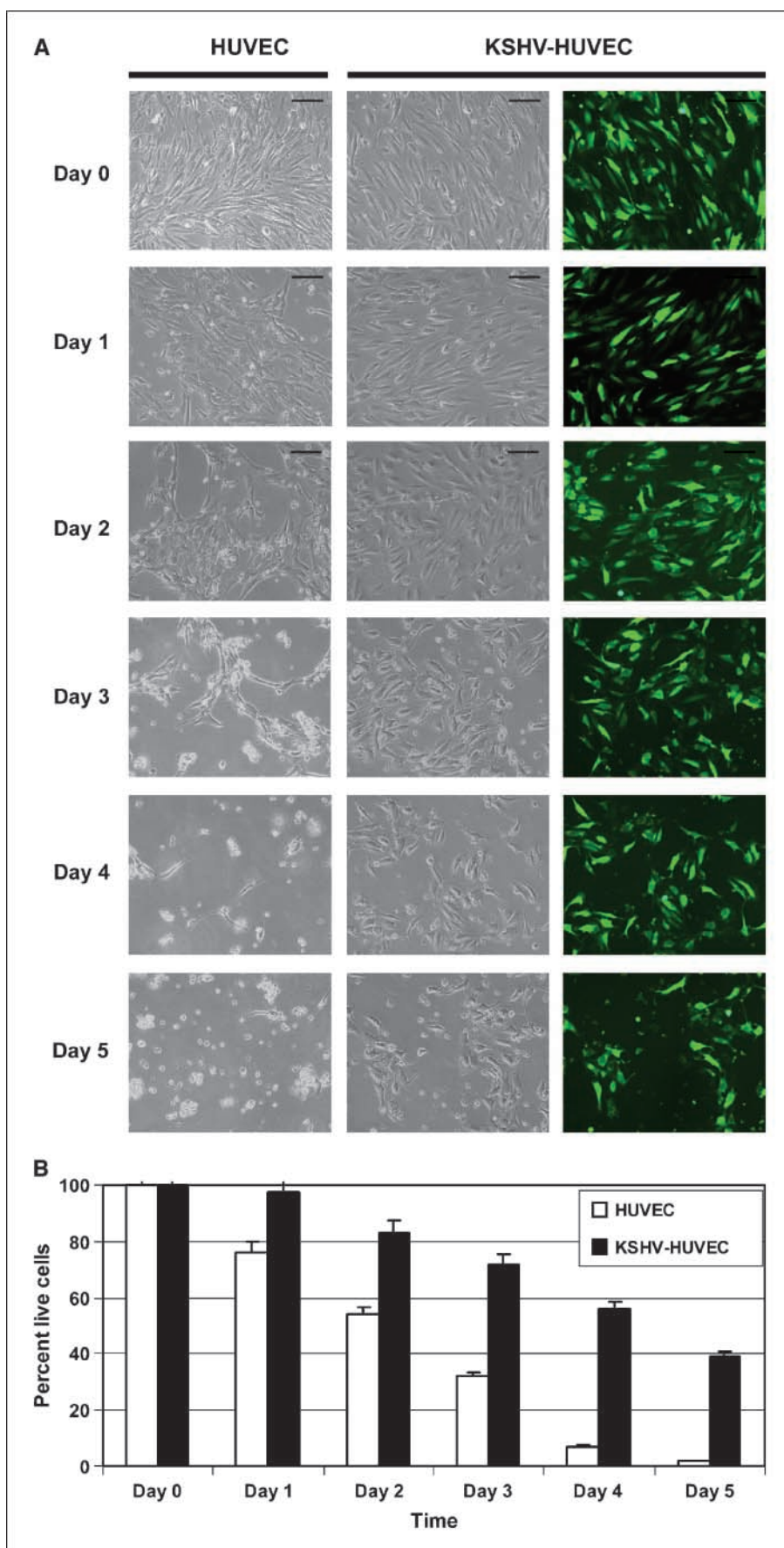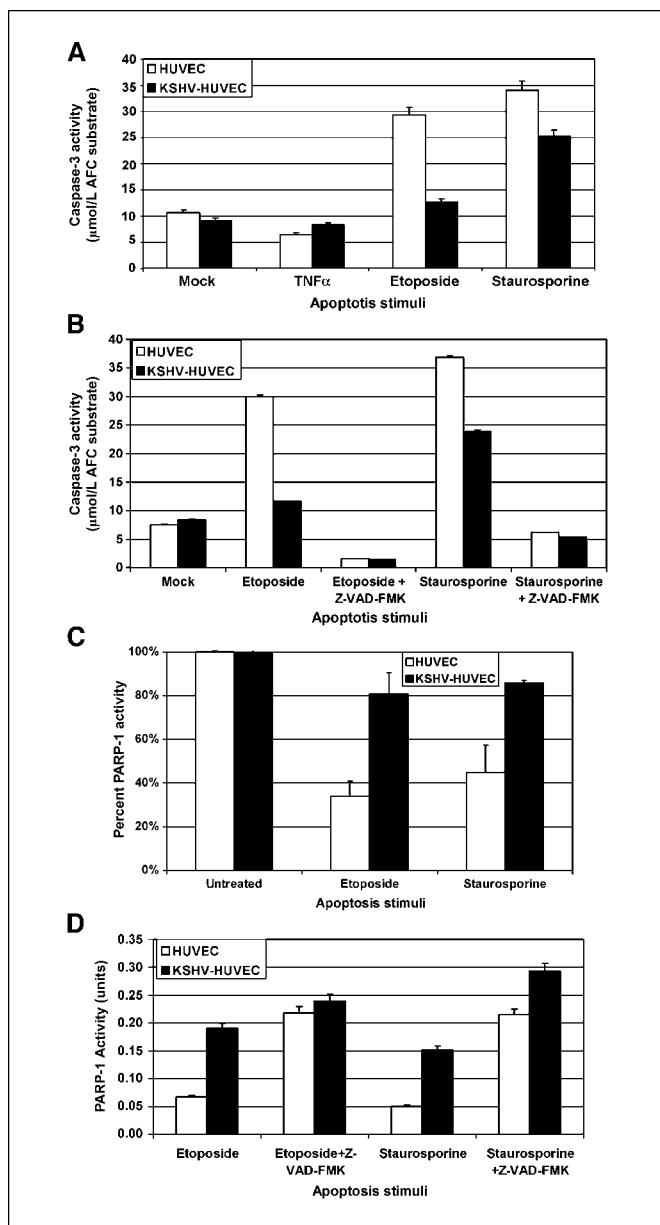
Figure 3. KSHV infection suppresses apoptosis induced by etoposide and staurosporine. *A,* HUVEC and KSHV-HUVEC were treated with endothelial medium, EBM-2, containing 500 ng/mL TNFα, 100 μmol/L etoposide, or 20 nmol/L staurosporine for 24 h. Cells were then harvested and caspase-3 activity was measured using the caspase-3 substrate, DEVD-AFC. Etoposide and staurosporine, but not TNFα, induced caspase-3 activation in the HUVEC and KSHV-HUVEC. However, caspase-3 activity induced in KSHV-infected HUVEC was lower than that induced in uninfected HUVEC. *B,* HUVEC and KSHV-HUVEC were incubated in EGM-2 medium containing 10% FBS, with either 100 μmol/L etoposide, 100 μmol/L etoposide plus 50 μmol/L Z-VAD-FMK, 20 nmol/L staurosporine, or 20 nmol/L staurosporine plus 50 μmol/L Z-VAD-FMK for 24 h. Cells were then harvested and caspase-3 activity was measured as above. Z-VAD-FMK, a caspase-3 inhibitor, dramatically suppressed caspase-3 activity induced by etoposide and staurosporine in HUVEC and KSHV-HUVEC. *C,* HUVEC and KSHV-HUVEC were incubated in EBM-2 medium, containing either 100 μmol/L etoposide or 20 nmol/L staurosporine for 24 h. Cells were then harvested and PARP-1 activity was measured using a colorimetric PARP assay kit (Trevigen). KSHV-HUVEC treated with etoposide maintained higher PARP-1 activity compared with uninfected HUVEC. *D,* HUVEC and KSHV-HUVEC were incubated in EGM-2 medium containing 10% FBS, with either 100 μmol/L etoposide, 100 μmol/L etoposide plus 50 μmol/L Z-VAD-FMK, 20 nmol/L staurosporine, or 20 nmol/L staurosporine plus 50 μmol/L Z-VAD-FMK for 24 h. Cells were then harvested and PARP-1 activity was measured as above. Z-VAD-FMK dramatically increased PARP-1 activity in HUVEC and KSHV-HUVEC stimulated with etoposide and staurosporine.

Matrigel contains significantly lower levels of stimulatory cytokines and growth factors, which allowed us to compare infected and uninfected HUVEC without the complications of high levels of cytokines in the medium. HUVEC and KSHV-HUVEC were plated on Matrigel and allowed to form tubule networks. We found that the KSHV-infected HUVEC formed more tubule structures than uninfected HUVEC within a 24-hour period (Fig. 4*A*).

KSHV is associated with KS, a tumor of endothelial origin, and PEL, a tumor of B-cell origin. We wanted to investigate whether the medium from KSHV-positive B-cell lymphomas could sustain endothelial tubule formation of KSHV-infected HUVEC. BJAB is a KSHV-negative B-cell lymphoma and BCBL-1 is a KSHV-positive B-cell lymphoma. We cultured the two cell lines in plain medium without serum for 48 hours and then harvested the medium for endothelial tubule formation assays to see whether HUVEC and KSHV-HUVEC could form tubules in the presence of the conditioned medium from these two B cells. We found that uninfected HUVEC could not form any tubule networks in either plain medium without serum or the conditioned medium collected from BJAB cells (Fig. 4*B* and *C*). In contrast, KSHV-HUVEC formed a branching network of tubules to a significantly greater extent than uninfected HUVEC in BJAB conditioned medium (Fig. 4*B* and *C*). Furthermore, the conditioned medium from the KSHV-positive PEL (BCBL-1) amply supported capillary-like tubule formation of KSHV-HUVEC (Fig. 4*B* and *C*). The KSHV-HUVEC tubules formed in the conditioned BCBL-1 medium were also more intact compared with KSHV-HUVEC tubules formed in either plain medium without serum, or the conditioned medium from BJAB cells. The uninfected HUVEC formed a couple of tubular structure in the presence of BCBL-1 cells but to a significantly lesser degree than KSHV-HUVEC. This suggests that KSHV-positive BCBL-1 cells secrete proangiogenic cytokines and growth factors that enhance the angiogenesis associated with endothelial cells, and to a greater degree with KSHV-infected endothelial cells.

KSHV-infected endothelial cells form tubules in the absence of exogenous VEGF and bFGF. VEGF and bFGF are two important growth factors involved in endothelial cell proliferation and angiogenesis. Many groups have reported that infection of endothelial cells with KSHV results in increased production of VEGF (45, 46). We have also found that KSHV-HUVEC secreted more VEGF than uninfected HUVEC (data not shown). We performed tubule formation assays in the absence of VEGF or FGF to determine if deprivation of these growth factors affects endothelial cell tubule formation over a 4-day time course. We found that at 24 hours after seeding the cells on Matrigel, both HUVEC and KSHV-HUVEC formed networks of tubules in complete EGM-2 medium, VEGF-minus EGM-2 medium, and bFGF-minus EGM-2 medium (Fig. 5*A*). By day 2, some of the tubules formed by HUVEC and KSHV-HUVEC in complete medium were broken; however, most of them were maintained very well, and there was no significant difference between the two cell lines (Fig. 5*A*). However, in the VEGF-minus EGM-2 medium and the FGF-minus EGM-2 medium, there were a significantly greater number of uninfected HUVEC tubules that were broken. In contrast, more intact tubules could still be visualized in the KSHV-HUVEC cells incubated in VEGF-minus EGM-2 medium or FGF-minus EGM-2 medium (Fig. 5*A*). By the 3rd day, most of the uninfected HUVEC died and almost all of the tubules were disintegrated. In contrast, we still found some intact tubular structures in the KSHV-HUVEC sample (Fig. 5*A*). Finally, on day 4, almost all of the uninfected HUVEC were dead but a proportion of the KSHV-HUVEC cells were still expressing GFP and formed tubules to some extent (Fig. 5*A*). Thus, KSHV infection of HUVEC confers a

survival advantage and helps maintain the endothelial tubular network under conditions of growth factor deprivation.

Because we and others have previously reported that KSHV infection of endothelial cells results in VEGF up-regulation, we next determined whether VEGF production by KSHV-HUVEC contributes to the increased angiogenesis seen with these cells. Hence, we performed the above tubule assays with HUVEC and KSHV-HUVEC in serum-free EBM-2 medium containing a blocking anti-VEGF antibody (20 μg/mL). We found that in the presence of the anti-VEGF antibody, there were hardly any tubules formed by the uninfected HUVEC (Fig. 5*B*). Although significantly inhibited, the KSHV-infected HUVEC still managed to form a very small number of tubules in the presence of the VEGF blocking antibody (Fig. 5*B*), suggesting that KSHV-HUVEC continuously secrete more VEGF and all of it is not completely blocked by the antibody.

NF-κB and PI3K pathways are essential for tubule formation by KSHV-HUVEC. We next determined the cellular pathways that are important for KSHV angiogenesis *in vitro*. We used a series of drug inhibitors to treat the endothelial cells in our tubule assays to determine which signaling pathways may play a key role in endothelial cell tubule formation and angiogenesis. In the presence of DMSO vehicle control, 2.5 μmol/L SU6656 (Src inhibitor; ref. 29), or 20 μmol/L piceatannol (Syk inhibitor; ref. 30), both HUVEC and KSHV-HUVEC formed tubule networks (Fig. 6*A*), implying that the Src and Syk signal transduction pathways are not necessary for HUVEC or KSHV-HUVEC angiogenesis *in vitro* under these conditions.

We also tested the importance of AMPK and mTOR signaling in tubule formation (Fig. 6*A*). We found that activation of AMPK by 150 μmol/L ciglitazone or inhibition of mTOR by 50 nmol/L rapamycin completely disintegrated the HUVEC cells and reduced the number of tubules formed by the KSHV-HUVEC (Fig. 6*A* and *B*). The same was true when we used 1 μmol/L rapamycin (data not shown).

Interestingly, 5 μmol/L Bay11-7085 (NF-κB inhibitor) treatment killed the HUVEC and KSHV-HUVEC and did not support tubule formation in either cell type (Fig. 6*A* and *B*). Furthermore, 20 μmol/L LY294002 (PI3K inhibitor) treatment resulted in a modest effect on the tubule formation of uninfected HUVEC, although most of the cells seemed unhealthy. In contrast, most of the KSHV-HUVEC died and could not form intact tubules with LY294002 treatment (Fig. 6*A* and *B*). These data suggest that the KSHV-HUVEC cells are more sensitive to inhibition of the PI3K signaling pathway than uninfected HUVEC. Thus, the NF-κB, PI3K, mTOR, and AMPK proteins are important for the viability and angiogenic properties of endothelial cells.

Discussion

To proliferate in an uncontrolled fashion, many cancer cells not only bypass cell cycle checkpoints but also inhibit apoptotic pathways, thereby ensuring their survival (see review by Bocchetta and Carbone in ref. 47). KSHV is associated with three different malignancies in the human population. In this report, we have evaluated the ability of KSHV to protect endothelial cells from different apoptotic stimuli.

It is well established that the PI3K/Akt signaling pathway regulates cell proliferation and cell survival (33). Here, we report that KSHV infection of endothelial cells induces activation of the PI3K and Akt kinases compared with uninfected cells. KSHV-infected cells also show a decreased activation of AMPK and an increase in phosphorylation and activation of mTOR. Previous studies have shown that two KSHV oncoproteins, vGPCR and K1,

activate the PI3K/Akt/mTOR signaling pathway in B cells and endothelial cells, and immortalize primary HUVEC (9, 18, 20, 21).

Because activation of the PI3K/Akt pathway has been linked to cell survival events, we investigated whether the KSHV-infected
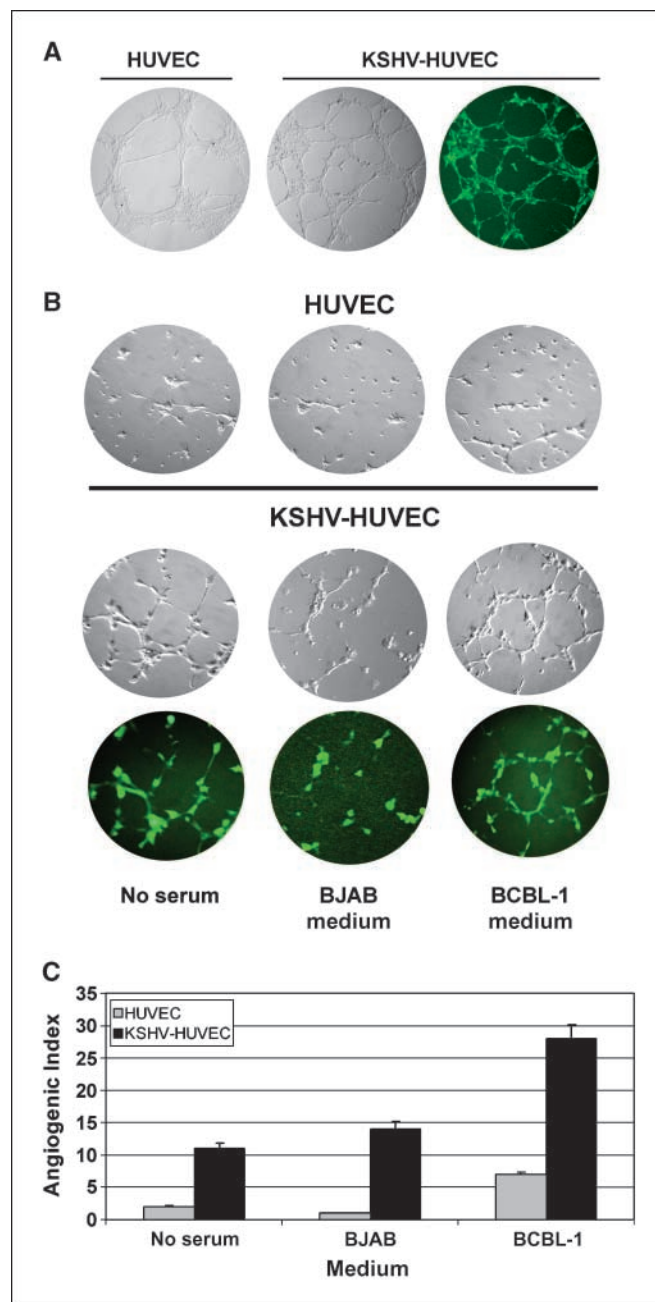

Figure 4. Tubule formation assay for HUVEC and KSHV-HUVEC. *A,* HUVEC and KSHV-HUVEC were plated on growth factor–reduced Matrigel in the presence of medium with serum for 24 h and allowed to form capillary-like tubules. *B,* KSHV-negative BJAB and KSHV-positive BCBL-1 cells were incubated in plain RPMI medium without serum for 48 h at 37°C, and then the conditioned medium from both cell lines was harvested for tubule formation assays. HUVEC and KSHV-HUVEC were seeded on Matrigel to form capillary-like tubules in the presence of medium without serum or conditioned medium from BJAB or BCBL-1 cells. Images of the HUVEC and KSHV-HUVEC cells were taken under bright field microscopy. Additionally, images of the KSHV-HUVEC (which express GFP) were taken under fluorescence microscopy. KSHV-HUVEC cells were capable of forming more tubules than the uninfected HUVEC under all three conditions. *C,* the angiogenic index, which reflects the number of branch points formed under each condition. The average number of branch points in five different fields per sample is shown.
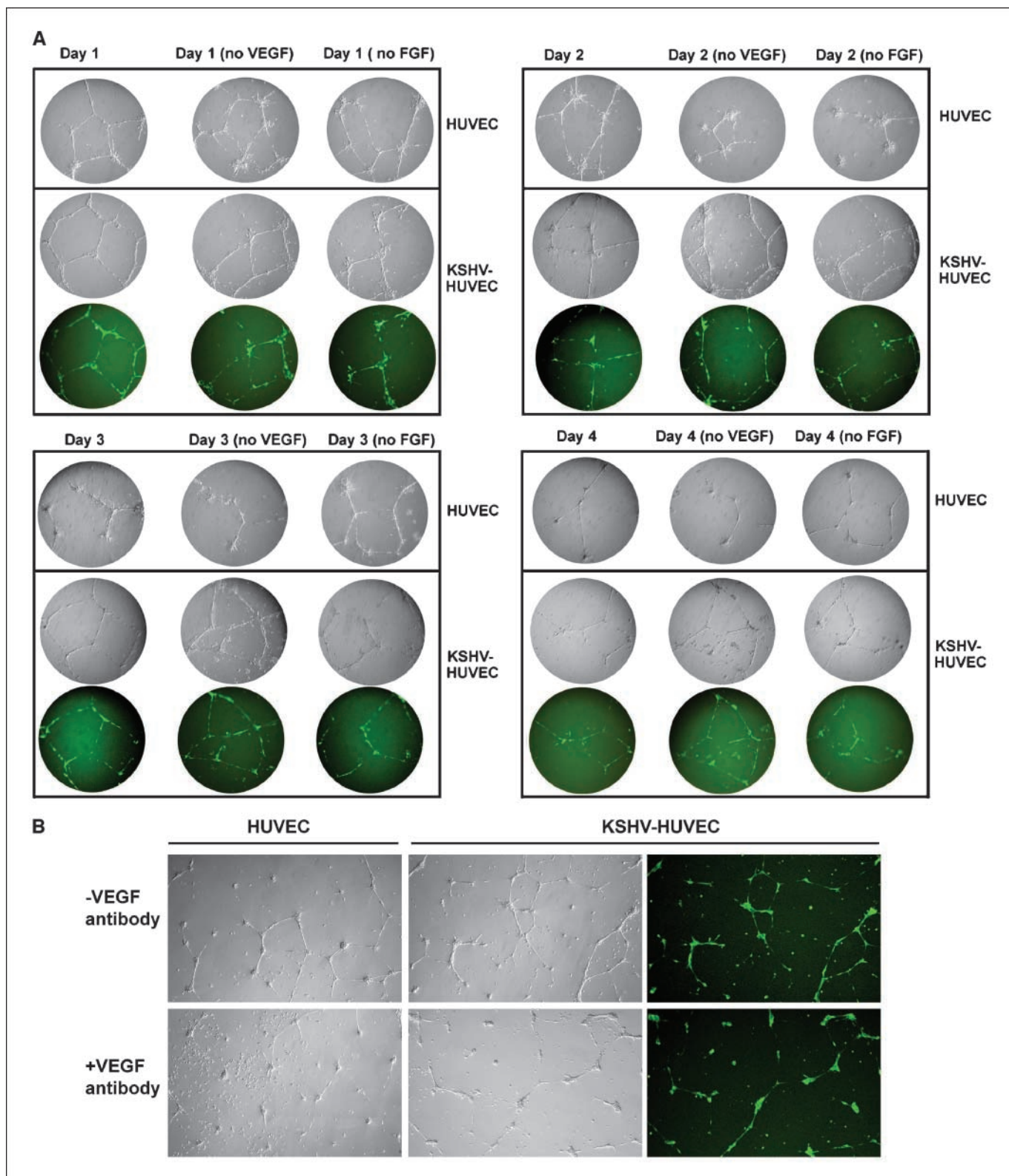
Figure 5. KSHV infection of endothelial cells allows tubule formation in the absence of VEGF and bFGF. *A,* tubule formation assays were performed with HUVEC and KSHV-HUVEC in endothelial cell complete medium, medium without VEGF, or medium without bFGF for 4 d. Images of the HUVEC and KSHV-HUVEC cells were taken under bright field microscopy. Additionally, images of the KSHV-HUVEC (which express GFP) were taken under fluorescence microscopy. The following time points were taken: 24 h, 48 h, 72 h, and 96 h. Images were taken at ×10 magnification. The tubules formed by KSHV-HUVEC were maintained on Matrigel for a longer period of time compared with those formed by HUVEC. *B,* tubule formation assays were performed with HUVEC and KSHV-HUVEC in serum-free EBM-2 medium, with or without anti-VEGF antibody. Images were taken after 16 h at ×4 magnification. Uninfected HUVEC could not form tubules in the presence of the blocking VEGF antibody. Although overall numbers of tubules were greatly reduced, KSHV-infected HUVEC could still form a few tubules in the presence of the blocking antibody.

cells had a cell survival advantage over uninfected cells under conditions of cell stress. We found that the KSHV-infected HUVEC were protected from serum starvation for a longer period of time compared with uninfected HUVEC and a significantly higher proportion of the KSHV-infected cells were alive 5 days after serum starvation compared with uninfected cells. Furthermore, the KSHV-HUVEC were more resistant to etoposide- and staurosporine-induced cell death compared with uninfected HUVEC as measured by caspase-3 and PARP-1 activity assays.

We also evaluated the ability of KSHV-infected cells to mediate angiogenesis under suboptimal conditions using *in vitro* tubule formation assays. In all experiments, KSHV-infected cells could form more tubules in the absence of serum, or in conditioned spent medium from KSHV-negative BJAB cells and KSHV-positive BCBL-1 cells, than uninfected HUVEC. This is likely because several KSHV viral proteins have been shown to increase VEGF expression and secretion (20, 23) and, hence, KSHV-infected cells may be less dependent on external growth factors than uninfected cells. Interestingly, in the presence of conditioned medium from BCBL-1 cells (and no exogenous growth factor addition), both uninfected HUVEC and KSHV-infected HUVEC could form tubules, with the latter forming a significantly higher number of tubules. KSHV-infected PEL have previously been shown to secrete cytokines and growth factors such as VEGF and IL-6 (8, 28) in the supernatant that likely facilitates this endothelial tubule formation.

Additionally, the KSHV-infected HUVEC could also form more tubules than uninfected cells when either VEGF or bFGF was removed from the endothelial cell medium or when a blocking VEGF antibody was added to the medium. Moreover, the KSHV-HUVEC maintained their tubule structures in the absence of VEGF or bFGF for a longer period of time (up to 4 days) compared with uninfected cells. It has previously been shown that KS lesions have high levels of expression of VEGF and bFGF and this suggests that VEGF secreted from infected cells contributes to endothelial cell survival and angiogenesis.

Finally, it seems that the PI3K and NF-κB pathways are critical for KSHV-induced tubule formation. We performed tubule formation assays in the presence of inhibitors of Syk, Src, PI3K, mTOR, and NF-κB, as well as an activator of AMPK. The Src and Syk inhibitors did not show any effect on the ability of the KSHV-HUVEC or uninfected HUVEC to form tubules. However, inhibitors of PI3K (LY294002), NF-κB (Bay11-7085), mTOR (rapamycin), and an AMPK activator (ciglitazone) either inhibited or reduced the ability of KSHV-HUVEC from forming tubules. NF-kB inhibition completely obliterated the KSHV-HUVEC and uninfected HUVEC from forming tubules, suggesting that this pathway is essential for angiogenesis. Interestingly, the PI3K inhibitor LY294002 reduced the ability of uninfected HUVEC to form tubules, but the KSHV-infected HUVEC were much more susceptible to PI3K inhibition, suggesting that these cells are highly dependent on PI3K activation. Weinstein and colleagues originally proposed the concept of oncogene addition in which cancer cells often rely on the activation of a specific signaling pathway. They suggest that inhibition of this specific pathway leads to preferential death of the cancer cell over a normal cell (48). A similar situation may be occurring in the KSHV-infected endothelial cells where they are more sensitive to PI3K inhibition than normal cells. This implies that therapeutic targets that inhibit members of the PI3K signaling pathway may be beneficial in the clinic against KS. Indeed, sirolimus (Rapamycin), which targets mTOR, the downstream effector of the PI3K and Akt kinases, has been shown to be efficacious against KS (28, 49). Further, we have recently published that rapamycin is also effective against PEL and can inhibit PEL cell
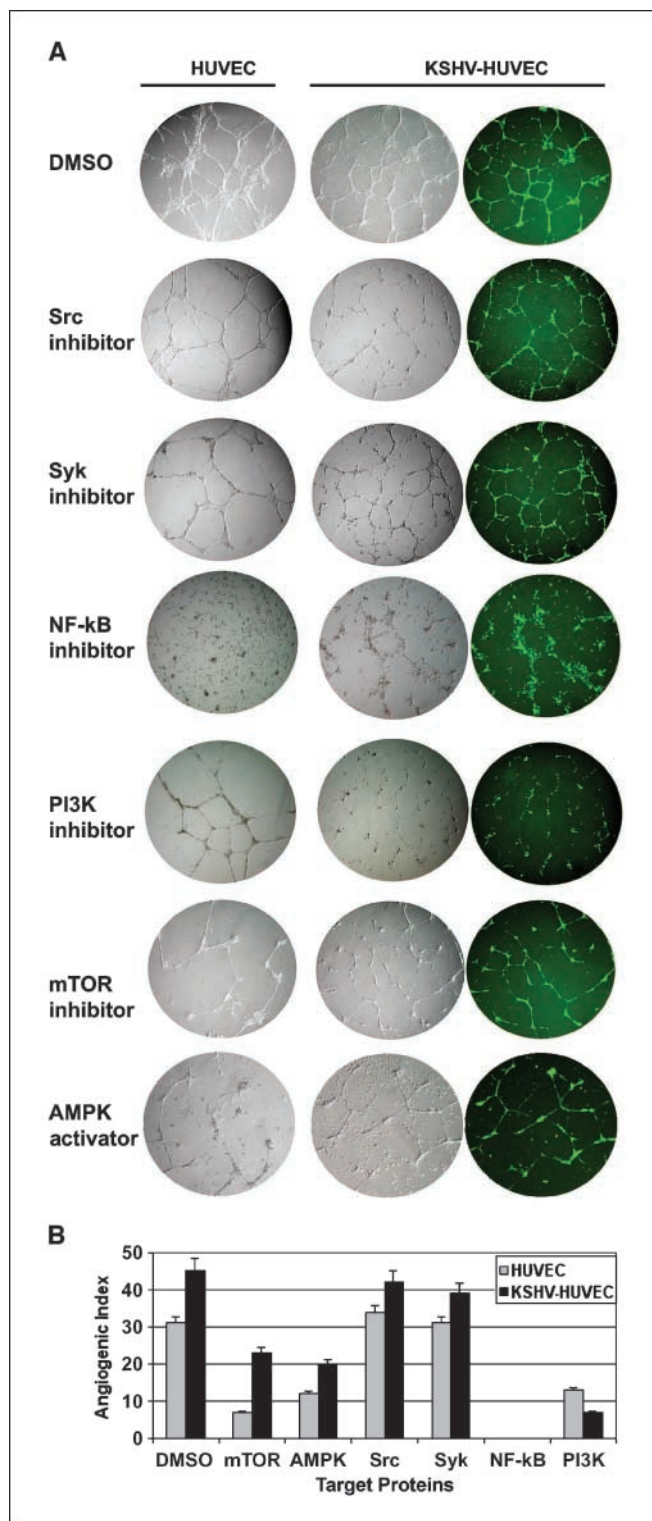

Figure 6. NF-κB and PI3K pathways are essential for tubule formation by KSHV-HUVEC. *A,* the tubule formation assays were performed on Matrigel with HUVEC and KSHV-HUVEC in EBM-2 medium containing 50 nmol/L rapamycin (mTOR inhibitor), 150 μmol/L ciglitazone (AMPK activator), 2.5 μmol/L SU6656 (Src inhibitor), 20 μmol/L piceatannol (Syk inhibitor), 5 μmol/L Bay11-7085 (NF-κB inhibitor), or 20 μmol/L LY294002 (PI3K inhibitor). Images of the HUVEC and KSHV-HUVEC cells under bright field were taken at 4 h. KSHV-HUVEC were also imaged under fluorescence microscopy. Images shown were taken at ×4 magnification. *B,* the angiogenic index, which reflects the number of branch points formed under each condition. The average number of branch points in five different fields per sample is shown.

growth *in vitro* and tumor formation in immunocompromised mice (28, 49). The data presented here show that the rapamycin inhibition of mTOR reduces the number of tubules formed by KSHV-infected HUVEC by 50%. Further, inhibition of the upstream kinase PI3K using LY294002 completely inhibited KSHV-HUVEC tubule formation. This suggests that inhibitors of the PI3K/Akt/mTOR pathway may prove efficacious against a broad spectrum of KSHV-associated cancers, including PEL and KS.

Taken together, our results provide compelling evidence that KSHV infection activates the PI3K/Akt/mTOR signaling pathway in endothelial cells and confers a cell survival and angiogenic advantage to these cells.

Disclosure of Potential Conflicts of Interest

No potential conflicts of interest were disclosed.

Acknowledgments

References

1. Chang Y, Cesarman E, Pessin MS, et al. Identification of herpesvirus-like DNA sequences in AIDS-associated Kaposi's sarcoma. Science 1994;266:1865–9.

2. Dupin N, Grandadam M, Calvez V, et al. Herpesvirus-like DNA sequences in patients with Mediterranean Kaposi's sarcoma. Lancet 1995;345:761–2.

3. Cesarman E, Chang Y, Moore PS, Said JW, Knowles DM. Kaposi's sarcoma-associated herpesvirus-like DNA sequences in AIDS-related body-cavity-based lymphomas. N Engl J Med 1995;332:1186–91.

4. Soulier J, Grollet L, Oksenhendler E, et al. Kaposi's sarcoma-associated herpesvirus-like DNA sequences in multicentric Castleman's disease. Blood 1995;86:1276–80.

5. Folkman J. Role of angiogenesis in tumor growth and metastasis. Semin Oncol 2002;29:15–8.

6. Samaniego F, Markham PD, Gendelman R, et al. Vascular endothelial growth factor and basic fibroblast growth factor present in Kaposi's sarcoma (KS) are induced by inflammatory cytokines and synergize to promote vascular permeability and KS lesion development. Am J Pathol 1998;152:1433–43.

7. Little RF, Yarchoan R. Treatment of gammaherpesvirus-related neoplastic disorders in the immunosuppressed host. Semin Hematol 2003;40:163–71.

8. Aoki Y, Tosato G. Role of vascular endothelial growth factor/vascular permeability factor in the pathogenesis of Kaposi's sarcoma-associated herpesvirus-infected primary effusion lymphomas. Blood 1999;94:4247–54.

9. Wang L, Dittmer DP, Tomlinson CC, Fakhari FD, Damania B. Immortalization of primary endothelial cells by the K1 protein of Kaposi's sarcoma-associated herpesvirus. Cancer Res 2006;66:3658–66.

10. Toker A. Protein kinases as mediators of phosphoinositide 3-kinase signaling. Mol Pharmacol 2000;57:652–8.

11. Kennedy SG, Kandel ES, Cross TK, Hay N. Akt/Protein kinase B inhibits cell death by preventing the release of cytochrome *c* from mitochondria. Mol Cell Biol 1999;19:5800–10.

12. Dudek H, Datta SR, Franke TF, et al. Regulation of neuronal survival by the serine-threonine protein kinase Akt. Science 1997;275:661–5.

13. Gingras AC, Kennedy SG, O'Leary MA, Sonenberg N, Hay N. 4E-BP1, a repressor of mRNA translation, is phosphorylated and inactivated by the Akt(PKB) signaling pathway. Genes Dev 1998;12:502–13.

14. Beevers CS, Li F, Liu L, Huang S. Curcumin inhibits the mammalian target of rapamycin-mediated signaling pathways in cancer cells. Int J Cancer 2006;119:757–64.

15. Nave BT, Ouwens M, Withers DJ, Alessi DR, Shepherd PR. Mammalian target of rapamycin is a direct target for protein kinase B: identification of a convergence point for opposing effects of insulin and amino-acid deficiency on protein translation. Biochem J 1999;344 Pt 2:427–31.

16. Inoki K, Li Y, Zhu T, Wu J, Guan KL. TSC2 is phosphorylated and inhibited by Akt and suppresses mTOR signalling. Nat Cell Biol 2002;4:648–57.

17. Hahn-Windgassen A, Nogueira V, Chen CC, Skeen JE, Sonenberg N, Hay N. Akt activates the mammalian target of rapamycin by regulating cellular ATP level and AMPK activity. J Biol Chem 2005;280:32081–9.

18. Tomlinson CC, Damania B. The K1 protein of Kaposi's sarcoma-associated herpesvirus activates the Akt signaling pathway. J Virol 2004;78:1918–27.

19. Sodhi A, Montaner S, Patel V, et al. Akt plays a central role in sarcomagenesis induced by Kaposi's sarcoma herpesvirus-encoded G protein-coupled receptor. Proc Natl Acad Sci U S A 2004;101:4821–6.

20. Bais C, Van Geelen A, Eroles P, et al. Kaposi's sarcoma associated herpesvirus G protein-coupled receptor immortalizes human endothelial cells by activation of the VEGF receptor-2/KDR. Cancer Cell 2003;3:131–43.

21. Sodhi A, Chaisuparat R, Hu J, et al. The TSC2/mTOR pathway drives endothelial cell transformation induced by the Kaposi's sarcoma-associated herpesvirus G protein-coupled receptor. Cancer Cell 2006;10:133–43.

22. Vieira J, O'Hearn PM. Use of the red fluorescent protein as a marker of Kaposi's sarcoma-associated herpesvirus lytic gene expression. Virology 2004;325:225–40.

23. Wang L, Wakisaka N, Tomlinson CC, et al. The Kaposi's sarcoma-associated herpesvirus (KSHV/HHV8) K1 protein induces expression of angiogenic and invasion factors. Cancer Res 2004;64:2774–81.

24. Wei MC, Zong WX, Cheng EH, et al. Proapoptotic BAX and BAK: a requisite gateway to mitochondrial dysfunction and death. Science 2001;292:727–30.

25. Vinci MC, Visentin B, Cusinato F, Nardelli GB, Trevisi L, Luciani S. Effect of vascular endothelial growth factor and epidermal growth factor on iatrogenic apoptosis in human endothelial cells. Biochem Pharmacol 2004;67:277–84.

26. Kirby JE, Nekorchuk DM. *Bartonella*-associated endothelial proliferation depends on inhibition of apoptosis. Proc Natl Acad Sci U S A 2002;99:4656–61.

27. Binetruy-Tournaire R, Demangel C, Malavaud B, et al. Identification of a peptide blocking vascular endothelial growth factor (VEGF)-mediated angiogenesis. EMBO J 2000;19:1525–33.

28. Sin SH, Roy D, Wang L, et al. Rapamycin is efficacious against primary effusion lymphoma (PEL) cell lines *in vivo* by inhibiting autocrine signaling. Blood 2007;109:2165–73.

29. Lannutti BJ, Blake N, Gandhi MJ, Reems JA, Drachman JG. Induction of polyploidization in leukemic cell lines and primary bone marrow by Src kinase inhibitor SU6656. Blood 2005;105:3875–8.

30. Lang ML, Chen YW, Shen L, et al. IgA Fc receptor (FcαR) cross-linking recruits tyrosine kinases, phosphoinositide kinases and serine/threonine kinases to glycolipid rafts. Biochem J 2002;364:517–25.

31. Ramanathan M, Pinhal-Enfield G, Hao I, Leibovich SJ. Synergistic up-regulation of vascular endothelial growth factor (VEGF) expression in macrophages by adenosine A2A receptor agonists and endotoxin involves transcriptional regulation via the hypoxia response element in the VEGF promoter. Mol Biol Cell 2007;18:14–23.

32. Dawson CW, Tramountanis G, Eliopoulos AG, Young LS. Epstein-Barr virus latent membrane protein 1 (LMP1) activates the phosphatidylinositol 3-kinase/Akt pathway to promote cell survival and induce actin filament remodeling. J Biol Chem 2003;278:3694–704.

33. Carpenter CL, Cantley LC. Phosphoinositide 3-kinase and the regulation of cell growth. Biochim Biophys Acta 1996;1288:M11–6.

34. Franke TF, Hornik CP, Segev L, Shostak GA, Sugimoto C. PI3K/Akt and apoptosis: size matters. Oncogene 2003;22:8983–98.

35. Porter AG, Janicke RU. Emerging roles of caspase-3 in apoptosis. Cell Death Differ 1999;6:99–104.

36. van Maanen JM, Retel J, de Vries J, Pinedo HM. Mechanism of action of antitumor drug etoposide: a review. J Natl Cancer Inst 1988;80:1526–33.

37. Matsumoto H, Sasaki Y. Staurosporine, a protein kinase C inhibitor interferes with proliferation of arterial smooth muscle cells. Biochem Biophys Res Commun 1989;158:105–9.

38. Tamaoki T, Nomoto H, Takahashi I, Kato Y, Morimoto M, Tomita F. Staurosporine, a potent inhibitor of phospholipid/Ca^{2+}dependent protein kinase. Biochem Biophys Res Commun 1986;135:397–402.

39. Pohlman TH, Harlan JM. Human endothelial cell response to lipopolysaccharide, interleukin-1, and tumor necrosis factor is regulated by protein synthesis. Cell Immunol 1989;119:41–52.

40. Dixit NM, Layden-Almer JE, Layden TJ, Perelson AS. Modelling how ribavirin improves interferon response rates in hepatitis C virus infection. Nature 2004;432:922–4.

41. Cooper JT, Stroka DM, Brostjan C, Palmetshofer A, Bach FH, Ferran C. A20 blocks endothelial cell activation through a NF-κB-dependent mechanism. J Biol Chem 1996;271:18068–73.

42. Satoh MS, Lindahl T. Role of poly(ADP-ribose) formation in DNA repair. Nature 1992;356:356–8.

43. Duriez PJ, Shah GM. Cleavage of poly(ADP-ribose) polymerase: a sensitive parameter to study cell death. Biochem Cell Biol 1997;75:337–49.

44. Staton CA, Stribbling SM, Tazzyman S, Hughes R, Brown NJ, Lewis CE. Current methods for assaying angiogenesis *in vitro* and *in vivo*. Int J Exp Pathol 2004;85:233–48.

45. Masood R, Cesarman E, Smith DL, Gill PS, Flore O. Human herpesvirus-8-transformed endothelial cells have functionally activated vascular endothelial growth factor/vascular endothelial growth factor receptor. Am J Pathol 2002;160:23–9.

46. Mutlu AD, Cavallin LE, Vincent L, et al. *In vivo*-restricted and reversible malignancy induced by human herpesvirus-8 KSHV: a cell and animal model of virally induced Kaposi's sarcoma. Cancer Cell 2007;11:245–58.

47. Bocchetta M, Carbone M. Epidemiology and molecular pathology at crossroads to establish causation: molecular mechanisms of malignant transformation. Oncogene 2004;23:6484–91.

48. Weinstein IB. Cancer. Addiction to oncogenes—the Achilles heal of cancer. Science 2002;297:63–4.

49. Stallone G, Schena A, Infante B, et al. Sirolimus for Kaposi's sarcoma in renal-transplant recipients. N Engl J Med 2005;352:1317–23.